Design parameters for the housing of two-dimensional air flow sensors

Reiner Jedermann, Nico Hartgenbusch, Mykhailo Borysov and Walter Lang

Abstract—**Micro machined sensors for the two-dimensional measurement of air flow magnitude and direction achieve very high sensitivity. The housing required for the protection of the sensor membrane greatly reduces the sensitivity for low velocities and induces deformation of the angle response. The first critical design factor is the gap height between the sensor surface and the protecting cover plate. The second is the layout of the necessary mounting bars to hold the cover. Several laboratory tests were conducted to evaluate and compare the influence of these factors. Best results were achieved by replacing the initial 4 needles holding the cover with a high number of wedge-shaped fins. The final sensor with improved housing was able to measure air flow in cooled fruit warehouses between 0.1 m/s and 2 m/s with a 2% deviation from an ideal sinusoid angle dependency.**

Index Terms—**anemometer, airflow profiling, flow sensor, sensor housing, wind sensor.**

I. INTRODUCTION

TWO-dimensional anemometers measure the magnitude and direction of air flow in a plane, typical applied as a wind sensor. Replacing large mechanical and moving components by a micro-fabricated chip has been discussed since 1974 [2]. Recently developed sensor elements operate according to the calorimetric principle, with at least three temperature sensors grouped around a resistive heater. Exposure to an external air flow creates a temperature gradient on the chip surface. The components of the air flow vector can be estimated from the temperature difference between opposing sensors. For the alternate hot-wire principle, resistors on the surface of a silicon chip or on a thin foil are used as both heater and sensor. A good overview of micro-machined sensors can be found in [3]. Two-dimensional anemometers are currently used in several new applications, including the navigation of drones and other flying objects [4] as well as the monitoring of air flow inside cooled warehouses [5].

A. Challenges in housing design

These applications impose new requirements on the housing design of the sensor system. Where traditional wind sensors for weather stations have fewer restrictions in size, now the size becomes critical for new applications, such as compact wind monitoring stations based on wireless sensor networks. The network can be used to monitor wind distribution in urban areas, or be applied in refrigerated warehouses to measure air flow inside gaps between boxes.

Especially within industrial applications, the housing needs a cover plate to protect the sensor chip, forming an air channel of a specific gap height g between chip and cover. The connection type for the cover to the lower portion of the housing is critical. Vortices behind the mounting bars can reach sensitive areas of the chip and create severe peaks of the sensor signal at certain angles. In wind sensor applications, the effect is less dominant, due to higher velocities and turbulence, as well as changing flow directions. In other applications with lower velocities in constant directions, and less distance between mounting bars and sensor chip by smaller housing size, these peaks have to be minimized by suitable housing layout.

Otherwise, the measurements can be largely distorted as tests with our initial housing design showed. Peaks of up to 30% of the sensor signal were observed for a housing with 65 mm diameter, for wind tunnel velocities v_0 between 1 m/s and 2 m/s.

A further complication is caused by the non-linearity of the Navier–Stokes equation. If the air velocity is reduced to values lower than the typical range of wind sensors, the pattern of the flow field changes. Very little air flow penetrates the narrow gap between chip and cover, resulting in very poor sensitivity for $v_0 < 0.2$ m/s.

B. State of the art

Several 2D flow chips have been developed in recent years. Few have been tested in combination with housings or for low velocity ranges necessary for applications outside of wind sensors.

The first complete system was developed by the University Delft, Netherlands [6]. A silicon chip with four 6 mm × 6 mm thermophiles (TPs) was glued onto a 0.25 mm ceramic carrier and mounted in a 200 mm diameter housing with a gap of 30 mm. The sensor was tested for velocities 1 m/s < v_0 < 25 m/s. The open housing without a cover and mounting bars showed

very good accuracy with an average error of 1° in angle and 1% in amplitude. Installing the cover on 3 mm thick bars increased the error to 5° and 10%, respectively. Replacing the bars by a cage made of a fine metal screen was recommended to remove the error induced by the bars. However, a metal screen with sufficiently low air resistance is mechanically less stable and therefore not suitable in many applications.

A group from Nanjing, China fabricated a 7.8 mm × 7.8 mm sensor element with 4 TPs on the bottom side of a 0.3 mm ceramic substrate [7]. The housing had 48 mounting bars and a total diameter of approximately 150 mm according to a photo in the paper. The Sensor was tested for 3.5 m/s<v_0<50 m/s with a constant heating power of 100 mW. The TPs were not directly exposed to the environment for the two systems above. The thin ceramic substrate protects the TPs, but also reduces their sensitivity.

The highest sensitivity was provided by systems that had the thermal sensors on the surface exposed to the environment, thus achieving a measurement range down to 1 cm/s. A group from Austria [8] placed 8 germanium thermistors around a heater on a 6 mm × 3 mm silicon chip. A velocity measurement range of 0.025 m/s<v_0<3 m/s was found for the stand-alone chip without housing. The tests were conducted by placing a small one-dimensional 12 mm wide and 1 mm tall channel with constant volume flow rate directly on the chip in different angle positions.

Sensitivity below 1 cm/s was reported for a chip from Freiburg, Germany [4]; however, also in this case only the stand-alone chip without housing was tested. The chip also used germanium thermistors on a silicon substrate. This system provided low energy consumption at 0.177 mW and was suitable for wireless applications.

A wearable sensor, based on the hot-wire principle was developed by a group form Beijing, China [9]. Three platinum thermal elements were applied onto a 50 μm flexible substrate. An accuracy of 0.44 m/s for 2 m/s<v_0<20 m/s was achieved with an energy consumption of 100 mW.

A group from Pisa, Italy followed a completely different concept for the housing design of a wind sensor [10]. They measure the X- and Y-components of the velocity vector with two different channel systems engraved into a 2 cm diameter cylinder. The dependency of the air flow through a single channel from the wind direction deviated significantly from a sinusoid. For compensation, they connected 5 channels with angular offsets of zero, ±21° and ±53° to two internal cavities each. The air velocity was measured inside an additional channel connecting the two cavities by TPs. Simulations of the hydraulic conductance of the channels showed that deviations from a sinusoid can be reduced to 4%. The maximum error for estimating the flow vector was ±5° for the angle and 8% for the magnitude during laboratory tests over a range of 0.5 m/s<v_0<8 m/s.

The same authors provided in a later theoretical work [11] a proof that this approach is able to compensate deviations from a sinusoid over a wide range of Reynolds numbers and a better method to optimize the angular offsets by simulations based on the experimental pressure distribution around the surface of

a cylinder. The prediction, that the magnitude error can be reduced to 2.5% with 7 channels on each side, has not been experimentally verified yet.

C.   Reconstruction of air flow magnitude and angle

Estimation of the flow magnitude and angle from the thermistor signals is not as straight forward as for one-dimensional flow sensors. In praxis, the sensor outputs in the X- and Y-directions are not proportional to the related components of the external flow vector. In addition to this non-linearity and the influence of the housing, deviations of the angle-dependency from a sinusoid shape must be taken into account.

The angle-dependency is not only distorted by the effect of the mounting bars, but also by non-rotation-symmetric layout of sensor and circuit board. This is especially true if the sensor is integrated into a small measurement system, where non-symmetric thermal conductivities must be considered. These issues make the estimation of the air flow vector from the measurements more complicated, but not impossible under the condition that sufficient calibration points for different angles and velocities are provided.

The flow vector can be estimated by searching for the pair of magnitudes and angles with the lowest deviations from an interpolated plane of calibration values. A detailed description of this estimation method is beyond the scope of this paper and will be published separately.

Regarding the costs for mass production, only a limited number of calibration points can be provided. The critical question is therefore not whether the angle-dependency diverts from a sinusoid, but whether this function can be reconstructed by a limited number of calibration points.

D.   Example applications for cold-chain monitoring

In this paper, we analyze housing design challenges by the example of monitoring air flow between crates in a cold storage warehouse. Apples are cooled for up to six months after the harvest season consuming high amounts of energy. Beside the compressors, 40% of the total electrical energy is required to maintain air circulation in the warehouse using fans [12]. Tests have shown that ventilation can be reduced by 50% without affecting the quality of the apples [12]. Less ventilation also means less moisture and weight loss and, thus, a higher retail price. However, reducing the ventilation rate increases the risk of stagnant zones with insufficient air flow for cooling and removal of carbon dioxide. Therefore, it is necessary to monitor the air velocity not only at the fan outlet, but also at multiple locations within the warehouse to guarantee a minimum velocity of 0.1 m/s. The apples were stored in 0.75 m × 1 m × 1.2 m plastic crates in rows 6 m high. Air flow sensors were installed into 10 cm wide horizontal gaps between the rows.

Automated feedback control of ventilation rate requires a set of air flow sensors with the following characteristics:

- The sensors should be small enough to fit into the gaps between the crates.
- The housing should have high mechanical stability to

survive between apples crates with a weight of 300 kg.

- Wires should be avoided since the sensors must be placed while the warehouse is being filled.
- The sensor should have a sensitivity of 0.1 m/s and should also measure air flow direction in order to detect unwanted circulations and eddies inside the stack.

Commercial anemometers were not able to fulfil these requirements, due to housing size, measurement range, and too high energy consumption for wireless applications. Therefore, a novel sensor was developed for this specific application.

E.   Goal of this paper

The first tests with prototypes of our sensor [1] confirmed that housing was a critical design issue. Apart from [11], no systematic studies of the influence of housing were found. The study in [11] followed a different principle with separate channel systems for X- and Y-direction and cannot be applied to other approaches for wind sensing with orthogonal TPs or thermistors in the same channel.

The first goal of this paper is to fill this research gap by studying the influence of different housing parameters with a focus on the cold storage warehouse use-case.

The effect on deviations from an ideal sinusoid angle-dependency and on the sensitivity at low velocities due to the number, shape and size of mounting bars, as well as of the gap height between sensor and cover were tested. Secondly, it was necessary to define a criterion that predicted how the accuracy of the system was affected, if only a limited number of calibration points were available. Finally, recommendations for the housing design should be given for our use-case of feedback fan control.

The subsequent section describes the measurement setup including the wind tunnel. A short description of the wireless air flow sensor and the criteria for the evaluation of the system performance are given, along with the different housing types tested. The remaining sections list the results, discuss the implications and summarize the study.

II.   MATERIALS AND METHODS

Several housing variants were tested for different air flow angles and velocities.

A.   Wind tunnel

The tests were conducted in a wind tunnel (Fig. 1) with a cross section of 200 mm × 200 mm at the measurement chamber and a sucking fan at the outlet. The fan speed was controlled by an STM32 microprocessor board, which provided exact setting of the revolutions per minute. The inlet was equipped with a honeycomb structure of tubes with 5 mm diameter and 50 mm length as laminator followed by a funnel to further reduce turbulences.

The wind tunnel achieved stable air flow with very little fluctuations over time within the test range of 0.05 m/s$<v_0<$2.2 m/s. The standard deviation for repeated measurements with the same air flow magnitude v_0 and angle was calculated to test the stability (see results section).

A servomotor-driven turntable allowed for fully automated measurements over different angles and velocities. The measured TP signal differences in X- and Y-direction were averaged over a period of 20 seconds per fan and turntable setting.

The sensitivity of the air flow sensor system including housing was tested during the first round of measurements for velocities of 0.05 m/s$<v_0<$2 m/s with 90° angle steps. The smoothness of the angle dependency was tested for v_0=2m/s and total 108 angle steps of 3.33°.

During additional tests, three 40 mm × 8 mm × 8 mm U-profiles were placed as obstacles on the floor of the wind tunnel (Fig. 2), in order to create small turbulence and to test the influence on the measured air flow.

B.   Air flow sensor

Our in-house fabricated air flow sensor-board was used to test different housing variants. The board was based on our 2 mm × 2 mm sensor chip for two-dimensional measurements. The chip consisted of a central heater surrounded by 4 TPs [13]. According to the calorimetric principle, the flow in X- and Y-directions can be estimated by the signal difference of two opposing TPs. In order to achieve minimal energy consumption and consequently, a long battery life, the heater was excited with pulses of constant energy by capacitor discharge [14] resulting in a total energy consumption of 2.3 mW including signal amplifiers and microcontroller.

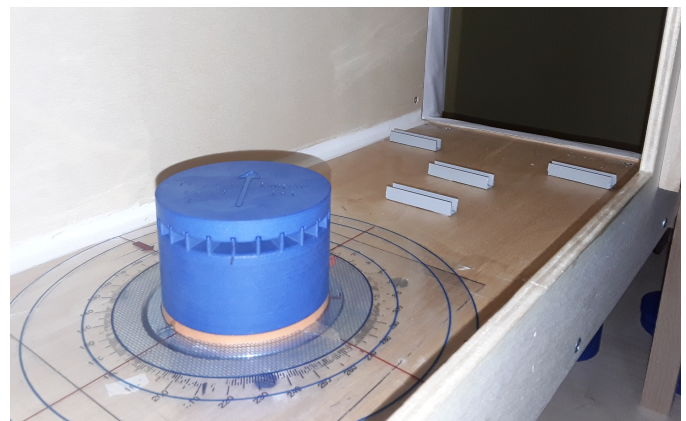Fig 1. Wind tunnel for air flow measurements

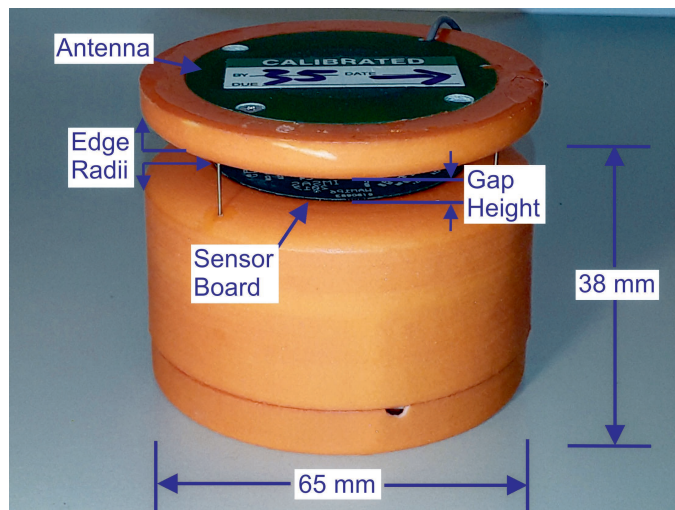Fig 2. Obstacles in the wind tunnel to create turbulence

Fig 3. Initial design of wireless anemometer with needles to hold the cover
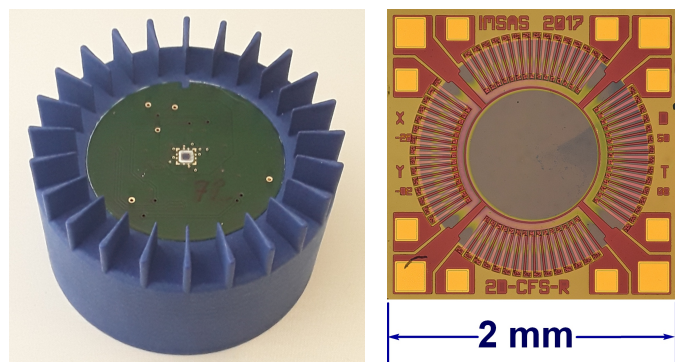

Fig 4. Current design and detailed view of 2D chip

The TPs react not with a continuous voltage difference, as in other driver circuits, but with a voltage pulse in the unit µV/s. Measurement data can be wirelessly transmitted using 868 MHz radio modules [15].

The complete sensor consisted of three printed circuit boards (PCB) with a diameter of 42 mm. The antenna PCB was integrated into the cover of the housing (Fig. 3). The sensor-board with chip and amplifiers was mounted below the gap in the housing. The radio-board and the battery were placed below the sensor-board and were not visible from the outside. The sensor-board was directly connected over a USB interface for easier handling during laboratory measurements, instead of using the radio-board.

Additional tests to compare the influence of different chip designs were carried out with an older 1D chip. Two chips were combined to provide 2D measurements. A small asymmetry in the board design could not be avoided; the two chips were displaced by 4 mm from the center of the sensor-board.

C.   Housing types and design parameters
The minimum housing size was determined by the diameter of the electronic boards and the required space for the battery. The housing had a fixed diameter of 65 mm and total height between 45 mm and 53 mm, depending on the gap height g

between sensor chip and cover plate. The housing parts were 3D printed by Oceanz, Netherlands.

In the initial housing design for the 2D chip, the cover was mounted using four 0.6 mm diameter needles. Tests with a gap of 3 mm$<g<$10 mm were described in an earlier publication [1]. Part of the test was repeated with the new 2D chip for g=3.5 mm and g=4 mm to maintain a consistent measurement setup and angle steps. In additional tests, the influence of the radii of the housing edges below and above the air gap (see Fig. 3) was investigated, as well as housings with 3 mm bars instead of needles.

For further tests, the 4 needles were replaced by a higher number of fins. The first series of fin housings was fabricated with fixed g=3.5 mm. The housings had either 16 or 36 rectangular or wedge-shaped fins of 10 mm length. The rectangular fins had a width of 1 mm. The outer side of the wedge fins was 1 mm wide and the inward side was 0.7 mm wide.

The second series of housings with 24 fins (Fig. 4) provided an option to vary the gap height in the range of 3 mm$<g<$8 mm using slots in the cover. Because of insufficient mechanical stability of thin fins in the first series, the outer width of wedge fins was increased to 1.5 mm. Further combinations of fin number, width and gap height were not tested, due to the high costs and required time for 3D fabrication.

The housing had a circumference of 204.2 mm. Between 7.8% and 17.6% of the air gap was covered by the outer side of the fins, whereas the 4 needles of the initial design covered only 1.2%.

D.   Definition of performance criteria
The first criterion used to compare the performance of different housing types was the magnitude of the TP signals for low velocities. In order to compensate for differences between the 1D and 2D chips, different gain factors of the sensor amplifier and variations in the chip manufacturing process, the TP signals were scaled in relation to the signal for a wind tunnel velocity of v_0=1 m/s.

The TP signals were measured for an angle of 0° and 180° in the Y-direction and 90° and 270° in the X-direction; i.e. the directions in which the TPs had the highest sensitivity. Benchmark values were calculated as the average TP signals for v_0=0.1 m/s and v_0=0.2 m/s in relation to v_0=1 m/s.

Two additional criteria were applied to quantify distortion of the angle dependency of the TP signals. The first test evaluated the deformation of the angle dependency in comparison with a sinusoid. Magnitude and angle offset of the sinusoid were fitted to all 108 measurements per velocity step. The benchmark 'sinusoid deformation' was defined as the root mean square error (RMSE) between sinusoid and measured value. The RMSE values for X- and Y-directions were averaged.

The third criterion tested how accurately the shape of the angle dependency could be reconstructed by a limited number of calibration points. The fitting function was estimated based on only 12 measurement points. A benchmark was calculated

as the RMSE between fitting function and all 108 measurement points. Because deformations with respect to a sinusoid were not critical in this step, a more advanced approximation method was used as fitting function.

The local polynomial regression (LPR) of order two fits the neighborhood of a target point with a parabolic function [16]. The approximation value was given as the value of the polynomial at the target location. The neighborhood with a range of $\lambda=\pm65°$ was weighted with a Tricube kernel function.

The latter two benchmarks were calculated for a wind tunnel velocity of $v_0=2$ m/s, because peaks and deformations of the angle dependency were more severe at higher velocities.

III. RESULTS

The TP signals showed good stability during 10 repeated tests at the same angle and velocity. The average standard deviation over different angles was 0.45% for $v_0=2$ m/s, and 1.4% for $v_0=0.2$ m/s in relation to the maximum TP signals.

Summaries of the results were plotted using Matlab in order to analyze the influence of parameters such as gap height and number of fins.

A.　Sensitivity for low velocities

Fig. 5 shows the absolute value of the TP response as a function of the wind tunnel velocity v_0 for the angles in which the TPs had the highest sensitivity. The two TP pairs showed good alignment for $v_0 \geq 0.2$ m/s, as well as the signal for positive and negative direction, with a standard deviation between 1.5% of the measured signal for $v_0=0.2$ m/s and 3.5% for $v_0=2$ m/s.

The problem of poor TP sensitivity for low velocities $v_0<0.3$ m/s, can be seen in the enlarged view in Fig. 6. The related non-linearity largely depends on the gap height g. For $g=3$ mm and $v_0<0.3$ m/s the curve had an almost parabolic shape, whereas the curve was nearly linear for $g \geq 5$ mm and 0.1 m/s$\leq v_0 \leq$0.5 m/s.

Deviations for higher velocities from an ideal linear relation are less critical. For $v_0 \geq 0.5$ m/s, the slope of the sensitivity function slightly decreased due to saturation effects (Fig. 6). The relation between gap height and sensitivity reversed for high velocities with the highest sensitivity for $g=3$mm at $v_0 \geq 1$ m/s. At high velocities, the air was more compressed by smaller gaps.

For a detailed analysis of the influence of the gap height and of the type of housing on the sensitivity for low air velocities, the TP signals were scaled in relation to their values for $v_0=1$ m/s. The relative sensitivity was plotted for $v_0=0.1$ m/s (Fig. 7) and $v_0=0.2$ m/s (Fig. 8).

For a small gap height of $g=3$ mm, all housing types had a similar relative sensitivity of ~1.3% for $v_0=0.1$ m/s and ~8% for $v_0=0.2$ m/s. The highest values and the largest increase with gap height were observed for the housings with needles and large radii on the edges at the air gap (red curves in Fig. 7 and 8) of 2 mm (height) × 32.5 mm (length). Decreasing the radii of the edges to 1 mm × 1 mm (magenta) also decreased the sensitivity by 11.5% on average.

The rectangular fins (black) had a slightly higher sensitivity than the wedge fins (blue) for the 24 fin design. Increasing the gap height to more than 5 mm negligibly increased the signal share for $v_0=0.2$ m/s. The measurements for 3 mm $\leq g \leq$ 4 mm showed that a higher number of fins led to a lower sensitivity.

The lowest sensitivity was measured for the initial sensor design with two separate 1D chips, which was 48% lower than for the 2D chip in the same housing with 4 needles (red hexagons).

B.　Smoothness of angle response

The signals of the TP pairs were measured for $v_0=2$ m/s at small angle steps and compared with a fitting sinusoid. Fig. 9 shows some example curves for the TP pair in Y-direction. The curves were scaled to the amplitude of the sinusoid of ±1 (yellow lines) and plotted with different vertical offsets in the same diagram for easier comparison. Verification tests at lower velocities showed that the measurements at $v_0=2$ m/s had the highest distortion.

The LPR reconstruction (dashed magenta lines) provided a good fit, even for the older 1D sensor with higher deformations from the sinusoid.
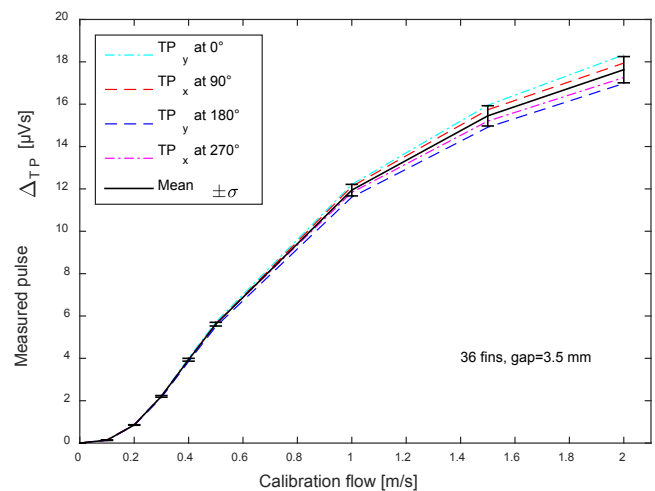

Fig. 5.　Thermopile response for air flow parallel to thermopile directions as function of velocity.
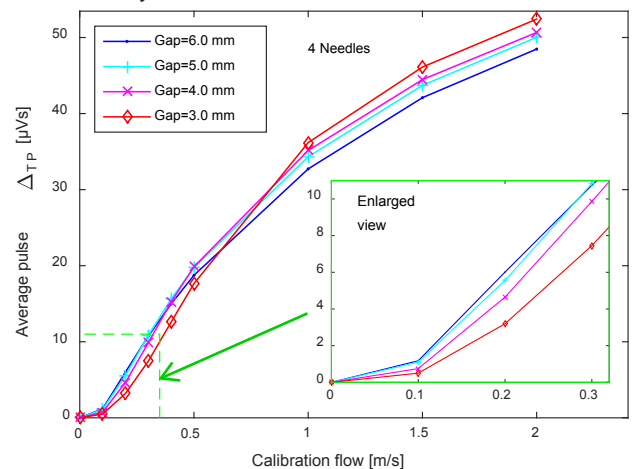

Fig. 6.　Measured sensitivity of thermopiles as function of gap height and velocity.
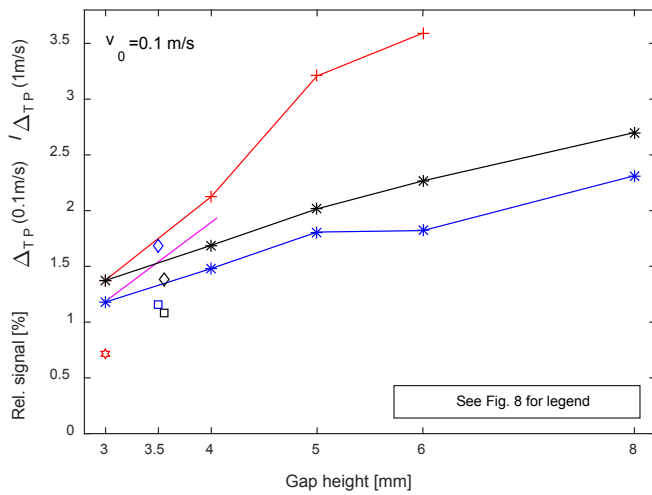
Fig 7. Relative sensitivity for v_0=0.1 m/s as function of gap height and housing type.
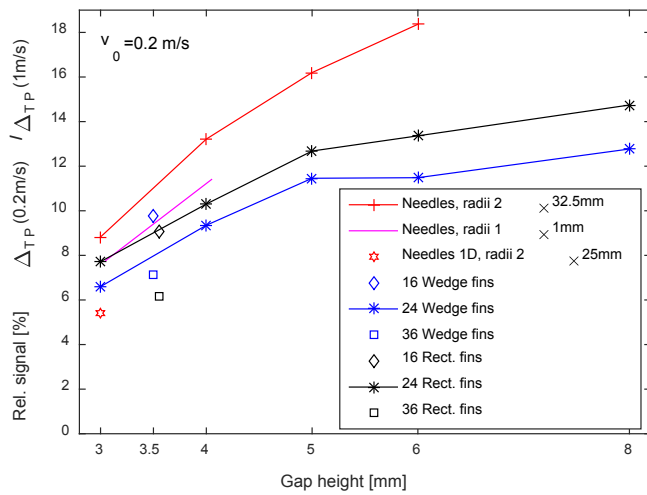

Fig 8. Relative sensitivity for v_0=0.2 m/s as function of gap height and housing type.

For the housings with 4 needles, the curve showed significant peaks at the needle positions (black line) with in average 11.6% of the sinusoid amplitude.

Compared with the first version of the sensor board with two separate 1D chips (dark blue) and peaks of 14.8%, the peak error was reduced by 1/5. If the 0.6 mm thick needles were replaced by 3mm bars (green) for the same sensor with a 2D chip, the RMSE more than doubled to 27.3%.

The lowest deformation of the curve with respect to a sinusoid was observed for the housing with 36 wedge fins (light blue). Housings with 24 fins and a higher gap showed some oscillations with a period equivalent to the distance of the fins in case of laminar flow (grey). If turbulence was induced in the wind tunnel by small obstacles, the oscillations nearly vanished (purple).

The influence of the edge radii were tested for the housings with needles. Reducing the radii from 2 mm (height) $\times$ 32 mm (length) to 1 mm $\times$ 1 mm also reduced the RMSE for the sinusoid fitting by 23.8% (not shown in figure).

For a detailed analysis, RMSE values for the deformations in relation to a sinusoid and for the reconstruction using only 12 calibration points based on LPR were calculated and plotted as a function of the number of fins (Fig. 10) and gap height (Fig. 11).

The error of the measured signal compared to the smoothed curve was always lower for the housing with fins compared with the 4 needles design. For the wedge-type fins, the error decreased monotonically with the number of fins. The error reduced by half to 1.96% for 36 fins for sinusoidal deformation, and by one third to 2.15% for the LPR reconstruction.

In order to estimate which share of the deformation was related to the housing itself and not to the mounting bars, the measurements at the needle positions were excluded.

If the RMSE was only calculated for angles that were not affected by obstacles, it decreased to 1.61% for the LPR reconstruction and to 3.17% for sinusoid deformation.
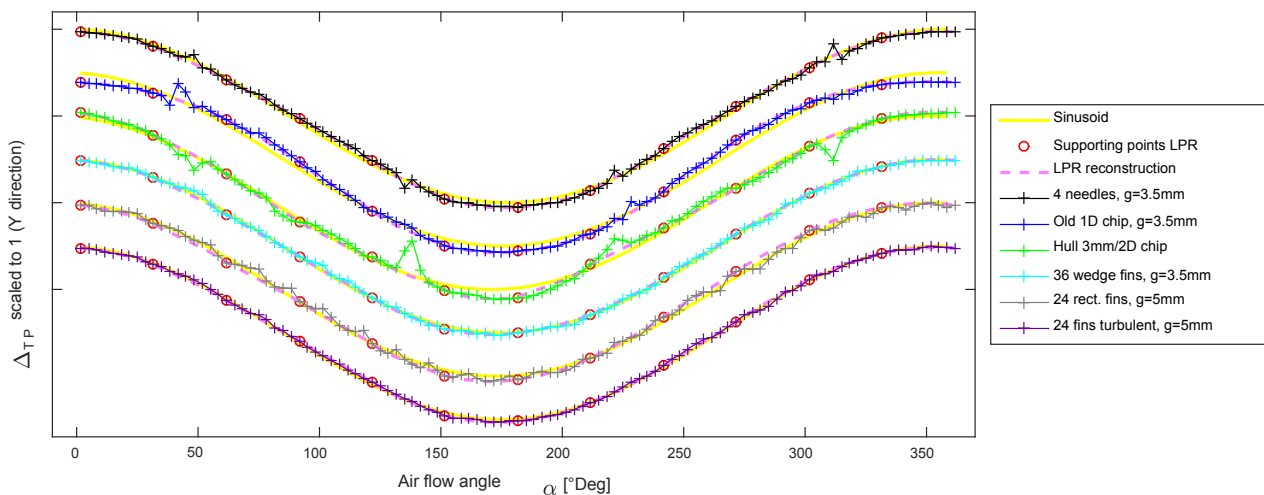

Fig 9. Measured angle dependency of the TP signals and fitting with sinusoid and LPR for v_0=2 m/s.
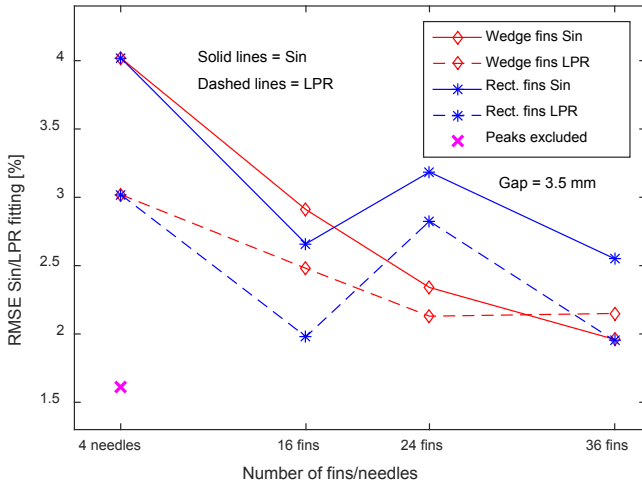
Fig. 10. Error of LPR reconstruction and sinusoid deformation as function of the number of fins, compared with 4 needles.
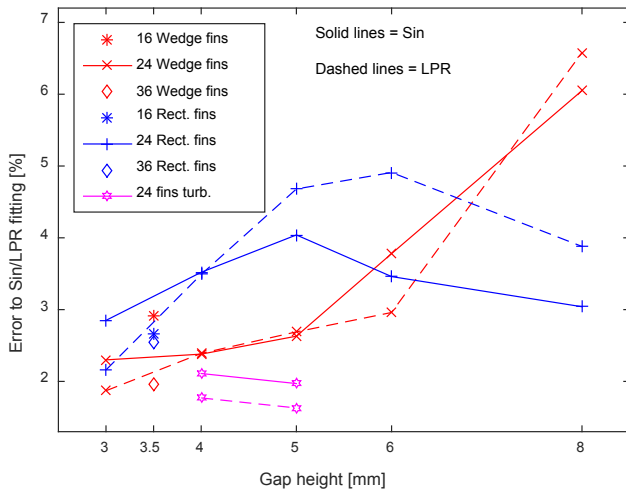

Fig. 11. Error of LPR reconstruction and sinusoid deformation as function of gap height.

The RMSE monotonically increased with gap height for wedge type fins, but more steeply for $g>5$mm (red lines in Fig. 11). Forcing turbulence by using small obstacles in the wind tunnel reduced the RMSE to a minimum value of 1.63% (magenta hexagons).

The LPR reconstruction was calculated based on 12 calibration points in 30° steps for each velocity. Using 9 calibration points in 40° steps increased the RMSE typically by a factor of 1.1, and using 6 points in 60° steps increased the RMSE by a factor of 1.75.

To directly compare sinusoid and LPR fitting, sinusoid fitting was also calculated based on 12 calibration points. In all cases, the RMSE of the sinusoid reconstruction was higher than those of the LPR reconstruction, on average by a factor of 1.3 (not shown in figure).

The RMSE for the rectangular fins showed irregularities with a higher error for 24 fins. The housings with 24 rectangular fins produced oscillations for $g=4$ mm and $g=5$ mm with higher RMSE. For larger gap heights, the RMSE decreased (blue).

C.   Angle error

The flow angle can be directly calculated from the X- and Y-measurements, if an ideal sinusoid shape of the calibration curves is assumed. The angle is given as the four-quadrant *arctan*() function of the relation between X- and Y-value, after correcting zero offsets and different amplifier gains of the two TP pairs. The resulting average and peak errors are given in Table I, as well as the percentage deviations from the sinusoid. The peak angle error was less than 5% for the wedge fin housings with $g\leq4$mm with an average angle error of 1.5%. Mounting the cover with needles resulted in 2times higher errors.

TABLE I: Average and peak angle error for V_0=2m/s and different housing types

Housing	Gap	Deviation sinusoid	Angle error
36 wedge fins	3.5 mm	1.96% / 6.7%	1.49° / 4.43°
24 wedge fins	4.0 mm	2.38% / 6.46 %	1.52° / 4.59°
4 needles	3.5 mm	4.02% / 14.02%	2.93°/ 9.60°

The estimation of the flow magnitude required an elaborate evaluation, due to the non-linearity of the TP sensitivity as function of magnitude. Using interpolated calibration curves instead of assuming a sinusoid increases the accuracy of the estimation, but also introduces a cross-sensitivity between the speed and the angle estimation. A description of the applied fitting method to relate the actual X- and Y-measurements to points on the interpolated planes of calibration curves for different velocities is beyond the scope of this paper. Initial tests with this method showed that the angle error for the fin housings can be reduced to 1.2° / 3° (average/peak). The magnitude error increased with the wind speed and reached an average of 0.1 m/s with peak errors of ±0.2 m/s for v_0=2m/s.

IV.   Discussion

A larger gap height resulted in a better sensitivity at low velocities, but also created more distortion in the angle response. Thus, the housing design must balance the two performance criteria of sensitivity and smoothness.

A.   Sensitivity

If a linear dependency between air flow and TP signal was assumed, the signal for v_0=0.1 m/s would be 10% of the signal for v_0=1 m/s. In practical measurements the relative sensitivity decreases to typically 1.3% for g=3 mm (Fig. 7), i.e. the sensitivity substantially drops for low velocities.

At low velocities, the air movement is dominated by friction forces versus inertial forces, as the latter decreases with the square of the velocity. In this sense, a detour around an obstacle is cheaper than through a narrow gap with high friction. This effect should be minimized by the housing design in order to provide sufficient sensitivity for low velocities.

The gap height was the design parameter with the highest influence. Up to g=5 mm, the sensitivity for v_0=0.1 m/s and v_0=0.2 m/s increased. If the gap was higher than $g>5$ mm, it only effected the sensitivity for v_0=0.1 m/s.

The edge radii of the housing had less influence. A larger radius directed more air into the gap by a funnel effect. This also increased distortions due to the eddies behind the needles or fins, resulting from a longer vertical length of such mounting bars being exposed to the air flow. A rather sharp edge with a 1 mm radius reduced the RMSE by 23.8%, and was therefore recommended, even though it also decreased the sensitivity by 11.5%.

The sensitivity of the housings with fins was lower than for the needle design, due to the higher share of the circumference covered by the front side of the fins. Furthermore, the air resistance was higher in the gaps between the fins.

For 16 and 36 fins, both rectangular and wedge variants had the same front width of 1 mm. Only the wedge variant with 24 fins had a higher front width of 1.5 mm, which led to a lower sensitivity than for the rectangular fins. The fins should be as thin as mechanical stability will allow. There were issues with the 1 mm wedge fins 3D printed in Polyamide-12, but no issues with the fins with 1.5 mm outer width. If the same material is used in the future, the outer fin width should be at least 1.2 mm.

B.   Smoothness

Even for a fictive case, when no needles or fins block the air flow, deformations compared with an ideal sinusoid angle dependency cannot be avoided. By excluding the needle positions, the sinusoid deformation was estimated to have an RMSE of 3.17%. Most of the deformations, which are due to asymmetries in the sensor and PCB design, were removed by switching to an LPR approximation. The RMSE reduced to 1.61%, even when only 12 calibration points were used for reconstruction.

The necessary mounting bars increased the RMSE. Needles entailed narrow and large peaks, but hardly affected the TP signals for angles between the needle positions. Fins created a smaller error affecting the whole angle range. For certain configurations, a periodic dependency of the RMSE on the fin positions was visible, but not regular enough to be compensated for by the model.

The peaks created by the **needles** depended on their diameter and the position of the sensor chip. The highest peak error was created by the 3 mm thick bars. The height of the peaks was reduced by using thinner needles, although this effect was limited by the aerodynamic boundary layer, with a thickness independent of the needle diameter.

In the earlier design with two separate 1D sensor chips, the location of the chips had an offset of 4 mm from the center of the housing and thus were closer to the needles, resulting in higher peaks and an offset between peak angle and needle position. A further disadvantage of the 1D chip was its 48% lower sensitivity (red hexagon in Fig. 7).

Peaks in the angle response made reconstruction of the air flow vector difficult and should therefore be avoided. The housings with fins did not show significant peaks. In general, the **wedge fins** showed the lowest error with an optimum for 24 or 36 fins and a gap height $g \leq 5$ mm with an RMSE<2.7% for LPR reconstruction using 12 calibration points in 30°

steps. Reconstruction by only 9 points in 40° steps was also possible, but the error increased by a factor of 1.1.

A definitive relationship between the outer width of the wedge fins and the smoothness could not be concluded from the measurements. However, it is expected that smaller fins will increase the smoothness.

The performance of the wedge fins was better than of the rectangular fins. The RMSE increased with the gap height. This was also confirmed by earlier measurements with needle housings and large gap heights. Only the **rectangular fins** made an exception for g=8 mm and 24 fins, with a decreasing RMSE (Fig. 11). The housing with 16 rectangular fins and g=3.5 mm also showed an unexpectedly low RMSE (Fig. 11).

C.   Blurring effects

If the air flow is fully laminar and without eddies behind an obstacle, the angle-dependency should show a sharp and high peak. However, in most housing designs, the peak was blurred by various effects; i.e. a wider angle range was affected at smaller amplitude. The concept of the Kármán vortex street [17] describes the formation of swirling eddies behind an obstacle. This effect can be increased by turbulence at sharp edges on the inward side of the fins.

A blurring effect of turbulence was verified by additional tests with small obstacles in the wind tunnel (Fig. 2). The obstacles created some turbulences and slightly fluctuating angle of air flow and, thus, largely reduced the RMSE (magenta lines in Fig. 11).

Most likely, the unexpected behavior of the rectangular fins can be explained by the turbulence effects. Although rectangular fins resulted in lower RMSE for some housing designs, this effect was rather unstable and could not be observed over a wide parameter range. Therefore we recommend using wedge fins, with more consistent test results.

Another factor that blurred the peaks caused by obstacles was the size of the sensitive area of the chip. Whereas the chip from Delft in [6] had a distance of 5 mm between the TP pairs, the distance was only 0.75 mm in our 2D chip. This explains the lower distortion reported in [6]. They measured a decrease of the sensor signal by -10% at the positions of the mounting bars, in our tests we measured increasing and decreasing magnitudes up to ±27% deviation.

V.   SUMMARY AND CONCLUSIONS

Wind sensors were the first application for 2-dimensional air flow meters. Because a wind sensor has practically no size limitation, large housings with sufficient distance between sensor surface and other mechanical components can be realized. In other practical applications, such as the measurement of air flow between crates in a cold store warehouse, the size of the housing is very limited. The geometrical layout of the housing then becomes a critical design factor. Distortions of the sensor signal with respect to flow magnitude and angle cannot be avoided, due to necessary compromises in the housing design.

The typical measurement range of wind sensors starts at several meters per second, whereas indoor air flow monitoring requires a range down to 0.1 m/s. If such a low range is necessary, the non-linearity of air flow in small gaps becomes problematic due to the insufficient sensitivity at low velocities.

The alternate housing concept with separate systems for X- and Y-direction with longer and narrow channels, presented in [10], only achieved a range down to 0.5 m/s. For our housing type, this non-linearity can be reduced by increasing the gap height. With a housing diameter of 65 mm, the gap height should not exceed 5 mm, otherwise distortions in the angle dependency for higher velocities become too large.

The necessary mounting bars to hold the sensor cover turned out to be the second problem. Best results were achieved when needles were replaced by a higher number of wedge-shaped fins. This entailed a moderate additional error in the angle dependency, but without large peaks. Furthermore, housings with fins had better mechanical stability and assembling the cover was easier.

It is necessary to consider not only the characteristics of the sensor chip, but also the complete system, including the housing. The new 2D chip showed considerable advantages over the earlier 1D chip, regarding both sensitivity and smoothness.

A reference TP signal for arbitrary angles was reconstructed using 9 or 12 calibration points per velocity step. Housings with 24 or 36 fins and a gap height between 4 mm and 5 mm achieved low reconstruction errors, with a RMSE<2.7%. In a direct comparison between the sinusoid and LPR fitting for reconstruction by a limited number of calibration points, LPR gave lower errors and was therefore preferred.

Tests with real housings in the wind tunnel showed much higher deviation and less sensitivity at low velocities than laboratory tests in literature with a small one-dimensional channel directly attached to the sensor-board.

The peaks in the angle-dependency caused by obstacles can be reduced by the above described blurring effects. However, these effects are not predictable and should therefore only be carefully applied; for example, by forcing turbulence using rectangular fins with sharp edges. Increasing the distance between the TPs or mounting the TPs on the bottom side of the substrate not directly exposed to the air flow also blurred peak distortion, but at the cost of decreasing the sensitivity of the chip.

Based on the considerations for housing design and a new 2D sensor chip, a wireless anemometer was constructed, for the required measurement range from 0.1 m/s to 2 m/s with sufficient accuracy, small form factor and low energy consumption.

This contribution showed that the housing of a two-dimensional air flow sensor is a critical design issue. Depending on the boundary conditions, such as the maximum housing diameter and the required measurement range, a specific design is necessary.

REFERENCES

[1] R. Jedermann, N. Hartgenbusch, M. Borysov, and W. Lang, "Housing design for two-dimensional air flow sensors," in *Proc. IEEE SENSORS 2017*, Glasgow, Scotland, 2017, pp. 1272-1274. doi: 10.1109/ICSENS.2017.8234300.

[2] A. Van Putten and S. Middelhoek, "Integrated silicon anemometer," *Electronics Letters,* vol. 10, pp. 425-426, 1974. doi: 10.1049/el:19740339.

[3] Y. Zhu, B. Chen, M. Qin, and Q. A. Huang, "2-D Micromachined Thermal Wind Sensors - A Review," *IEEE Internet of Things Journal,* vol. 1, pp. 216-232, 2014. doi: 10.1109/JIOT.2014.2319296.

[4] A. S. Cubukcu, E. Zernickel, U. Buerklin, and G. A. Urban, "A 2D thermal flow sensor with sub-mW power consumption," *Sensors and Actuators A: Physical,* vol. 163, pp. 449-456, 2010/10/01/ 2010. doi: 10.1016/j.sna.2010.08.012.

[5] R. Jedermann, N. Hartgenbusch, M. Borysov, C. Lloyd, U. Praeger, M. Spuler and W. Lang, "Spatial profiling of airflow conditions in cold storage warehouses by wireless anemometers " in *6th International Cold Chain Management Conference*, Bonn, Germany, 2016, pp. 93-98.

[6] B. W. V. Oudheusden and J. H. Huijsing, "Microelectronic Thermal Anemometer for the Measurement of Surface Wind," *Journal of Atmospheric and Oceanic Technology,* vol. 8, pp. 374-384, 1991. doi: 10.1175/1520-0426(1991)008<0374:mtaftm>2.0.co;2.

[7] Y. Zhu, B. Chen, F. Gu, M. Qin, and Q. Huang, "A self-packaged two-dimensional thermal wind sensor based on thermopiles for low cost applications," *Journal of Micromechanics and Microengineering,* vol. 24, p. 075008, 2014. doi:

[8] F. Keplinger, J. Kuntner, A. Jachimowicz, F. Kohl, and B. Jakoby, "Highly Sensitive Sensor for Flow Velocity and Flow Direction Measurement," in *2006 5th IEEE Conference on Sensors*, 2006, pp. 1436-1439. doi: 10.1109/ICSENS.2007.355903.

[9] S. Zhao, P. Jiang, R. Zhu, and R. Que, "Wearable anemometer for 2D wind detection," in *2016 IEEE SENSORS*, 2016, pp. 1-3. doi: 10.1109/ICSENS.2016.7808599.

[10] M. Piotto, G. Pennelli, and P. Bruschi, "Fabrication and characterization of a directional anemometer based on a single chip MEMS flow sensor," *Microelectronic Engineering*, vol. 88, pp. 2214-2217, 2011/08/01/ 2011. doi: 10.1016/j.mee.2010.11.009.

[11] P. Bruschi and M. Piotto, "Determination of the Wind Speed and Direction by Means of Fluidic-Domain Signal Processing," *IEEE Sensors Journal,* vol. 18, pp. 985-994, 2018. doi: 10.1109/JSEN.2017.2780521.

[12] D. Kittemann, R. McCormick, and D. A. Neuwald, "Effect of high temperature and 1-MCP application or dynamic controlled atmosphere on energy savings during apple storage," *European Journal of Horticultural Science,* vol. 80, pp. 33-38, 2015.

[13] N. Hartgenbusch, "A micromachined, membrane based, thermoelectric flow sensor for 2-dimensional measurement with high angular resolution," accepted for *IEEE Sensors Conference*, 2018.

[14] N. Hartgenbusch, M. Borysov, R. Jedermann, and W. Lang, "Reduction of power consumption and expansion of the measurement range by pulsed excitation of thermal flow sensors," *Sensors and Actuators A: Physical,* vol. 265, pp. 313-320, 2017. doi: 10.1016/j.sna.2017.08.029.

[15] R. Jedermann, M. Borysov, N. Hartgenbusch, S. Jaeger, M. Sellwig, and W. Lang, "Testing Lora for food applications - Example application for airflow measurements inside cooled warehouses with apples," *Procedia Manufacturing,* vol. 24, pp. 284-289, 2018/01/01/ 2018. doi: 10.1016/j.promfg.2018.06.026.

[16] T. J. Hastie, R. J. Tibshirani, and J. H. Friedman, *The elements of statistical learning: data mining, inference, and prediction*, 2nd ed.: Springer, New York, 2009.

[17] T. Von Kármán, *Aerodynamics: selected topics in the light of their historical development*: Courier Corporation, 2004.